Holographic Determination of Local Mass Transfer Coefficients at a Solid-Liquid Boundary

D. N. KAPUR and N. MACLEOD

Chemical Engineering Department
University of Edinburgh, Edinburgh, Scotland

We have described elsewhere (Kapur and Macleod, 1972, 1974) the use of holographic interferometry for measuring coefficients of mass transfer from a solid surface to air. Using a test body coated with silicone rubber initially swollen to equilibrium with an organic ester of suitable volatility, we have shown that the pattern of local recession corresponding to the spatial variation of mass transfer rate produced by the flow of air over the surface may be registered holographically with great exactitude and displayed in a panoramic manner with much wealth of detail.

We here demonstrate the extension of this unprecedentedly precise and powerful method to the measurement of mass transfer coefficients at a solid-liquid interface.

The principle of this essentially profilometric technique remains the same whether the experimental fluid is gas or liquid. Shrinkage of the coating due to transfer of the swelling agent to the fluid stream is arranged to bring about changes in the optical path length of rays of coherent light reflected from, or passing through, the coating, in an optical system capable of forming holograms of the experimental surface. Superimposition of such holograms obtained before and after exposure of the surface to the experimental fluid stream generates an interferogram or photographable array of interference fringes, loci of constant surface recession, revealing the entire pattern of change in the configuration of the surface and hence of the spatial variation of mass transfer rate over it. If the elastomer/swelling agent system is arranged to fulfill certain readily attainable physico-chemical conditions, this pattern of transfer rate variations is also the pattern of spatial variation of fluid-side transfer coefficient (Macleod and Todd, 1973). This can be revealed in its entirety in a single photograph with a precision and completeness not attainable by any other known method.

Silicone rubbers in general are not significantly swollen by water, which is therefore a suitable experimental fluid. Organic esters are readily available that are good swelling agents for these rubbers and also have sufficiently low solubilities in water to give a reasonably long constant-rate period (Macleod and Ruess). Salicylates are particularly suitable.

The calculation of absolute values of mass transfer coefficients from holographic measurements requires a knowledge of the solubility of the swelling agent in the experimental fluid. Published data on the solubility of organic esters in water are extremely scanty. We have therefore ourselves determined the solubility in water of ethyl salicylate, using a novel method introduced by Kapur (1973) and employed also by Macleod and Ruess. Ethyl salicylate was chosen as the swelling agent here because it has already been extensively used by us for swelling the polymer coatings used in determining local air-side mass transfer coefficients at solid surfaces and most of the relevant data for it are accurately known.

The diffusivity of the swelling agent in the experimental fluid must be known to allow the mass transfer results to be generalized in dimensionless form. The diffusion coefficient of ethyl salicylate in water has been determined by Macleod and Ruess from experiments on the laminar axial flow of water through an annulus between coaxial cylinders, the inner cylinder having a silicone rubber coating initially swollen to equilibrium in ethyl salicylate.

These experimentally determined values of solubility and diffusivity have been used to interpret and correlate the results of the experiments now to be described on the profilometric determination of mass transfer coefficients from a flat plate held normal to an impinging laminar submerged jet of water. These results have been compared with analytical predictions and experimental measurements of Scholtz and Trass (1963) for a similar system.

APPARATUS

The flat plate used in these experiments was 15.24 × 15.24 × 1.27 cm, made of alumium alloy and provided with 'hole, groove and ball' kinematic constraints similar to those described by Macleod and Kapur (1973), such that it could be precisely located on a kinematic mount placed on the optical table for the preparation of holograms. The plate was supported during the mass transfer experiments in a closed rectangular tank, shown in section in Figure 1, equipped with mounts comprising a hard steel bearing ball and a stainless steel cylinder designed to engage with the hole and groove constraints carried by the flat plate. A ball-ended screw passing through a tapped hole in one perspex face of the box was designed to bear against the ball constraint, pressed into a hole drilled in the back of the coated plate. This ball-ended screw, together with a screw mechanism capable of laterally traversing the stainless steel cylinder, enabled the coated plate to be set accurately normal to the jet of water issuing from the nozzle. The nozzle, a 35.6-cm length of stainless steel tubing (6.3-mm I.D.) was fixed through the other perspex side of the tank, and was supplied with water at a measured temperature from a gravity reservoir via a rotameter. The tank, which was closed with a tight fitting lid, was completely filled with water during the experiments. Water left the apparatus via an exit pipe fixed in the wall of the tank behind the specimen plate.

EXPERIMENTAL PROCEDURE

The diffusely reflecting aluminum plate, coated with a cast layer of transparent silicone rubber (EP411 from I.C.I. Ltd., Stevenston, Ayrshire), was immersed in ethyl salicylate until the coating was swollen to equilibrium. It was then superficially dried and was transferred to the kinematic mount which located it accurately on the optical table furnished with the standard equipment for making holographic interferograms by the transparent coating method (Method (11) of Kapur and Macleod, 1974). After the initial state of the coated plate had been recorded holographically, the plate was removed from the optical table and located in the tank, which was prepared almost full of water. Next, the perspex lid of the tank was bolted in position. Water of known temperature from the overhead

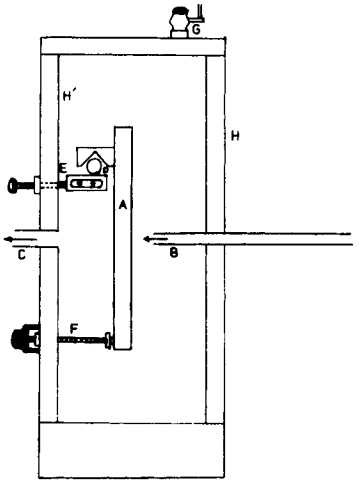

A - Specimen Plate
B - Jet Nozzle
C - Fluid Exit
D - Cylindrical Kinematic Constraint
E - Screw Mechanism
F - Ball-Plane Kinematic Constraint
G - Bleed Cock
H - Perspex Front
H' Perspex Back

Fig. 1. Cross-sectional side view of apparatus.

reservoir was then admitted through the nozzle, and air was quickly expelled from the tank via a bleed cock in the lid. The water flow rate was then measured by means of a rotameter. The run was terminated after a known period of time (generally a few minutes), chosen to fall within the calculated constant rate period for most of the plate surface—for the wall-jet region, in particular—under the conditions of the experiment. The plate was removed from the water tank and thoroughly dried by means of fine paper tissue, particular attention being paid to the complete drying of the kinematic constraints. After relocation of the coated plate on the optical table, a few minutes were allowed for equilibration to room temperature before the second exposure of the holographic plate was made, recording the hologram of the coated plate after mass transfer on the undeveloped photographic plate bearing the initial image. The doubly-exposed photographic plate was subsequently developed and fixed.

The runs were repeated for different Reynolds numbers.

RESULTS AND DISCUSSION

Interference fringes formed between the holograms of the coated plate made before and after exposure to the jet of water for known periods appeared as frozen-fringes on reconstruction of the double-exposed hologram.

Diameters of the sets of fringes obtained for different jet Reynolds numbers were measured from enlarged (x 1.5) photographs of the reconstructed interferograms. Measurements of pairs of orthogonal diameters for each fringe agreed to within 2% in all cases. The fringe order numbers for the fringes recorded on the photographs were found in the manner described by Kapur and Macleod (1974), by logarithmic plotting of the diameter measurements for the outermost fringes against integers of a consecutive set chosen to yield the form of functional relation predicted by the theory of Scholtz and Trass (1963) for the wall-jet region, that is, for the zone of flow beyond a certain distance from the jet axis.

The geometry of the optical system being known and values of the refractive index of the swollen coating having been measured (Kapur and Macleod, 1974), absolute mass transfer coefficients could be calculated when the solubility of ethyl salicylate in water was known. The solubility was determined from the measured loss in weight of rubber samples, initially swollen to equilibrium with ester, after prolonged immersion in known volumes of water in closed, stirred thermostatted flasks (Kapur, 1973; Macleod and Ruess). The assumptions that the final concentration of ester in the water was that corresponding to equilibrium with the ester within the rubber phase, and that this in turn was near equilibrium with the pure ester, were checked by confirming that the total weight loss was unaffected by variations in the duration of the experiment (usually about 24 hours) and by variations in the number of swollen rubber pieces in a given flask. The solubility of ethyl salicylate in water, thus measured, is plotted as a function of temperature in Figure 3.

The results obtained at jet Reynolds numbers in the range 1,000 to 3,000, expressed in dimensionless form with the aid of Scholtz and Trass' wall-jet correlation and Macleod and Ruess' data for the diffusivity of ethyl salicylate in water, are shown in Figure 4 as $Sh/Re^{0.75}\,Sc^{0.33}$ plotted against x/d. The solid line represents the theory of Scholtz and Trass for the wall-jet region. For the lowest values of Re, that is, 1055 and 1400, the agreement between this theory and the experimental data is good up to the line aa', the expected limit of Scholtz and Trass' theory. At higher values of Re, however, the conformity with the theoretical line becomes progressively less satisfactory, particularly as the limit aa' is approached, the discrepancy reaching a value of 17% in the worst case.

It appears likely that these regular deviations are attributable, not to a breakdown of Scholtz and Trass' theory, but to violation of the constant rate condition on which the experimental method depends. Calculation shows that for each experimental point showing an appreciable de-

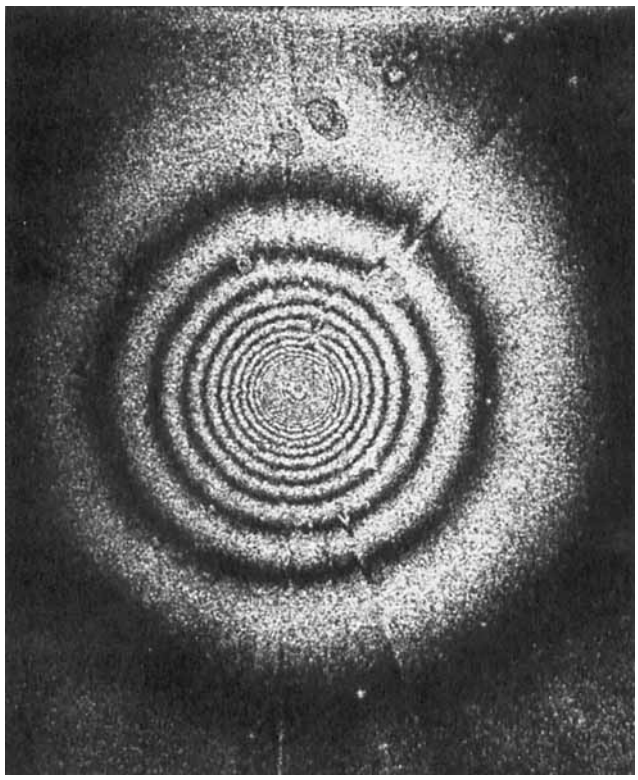

Fig. 2. Fringes obtained by holographic interferometry, recording mass transfer of ethyl salicylate from a silicone rubber coating on a flat plate exposed to a normal water jet ($Re = 1400$; $Sc = 1074$; nozzle to plate distance 15.9 mm).

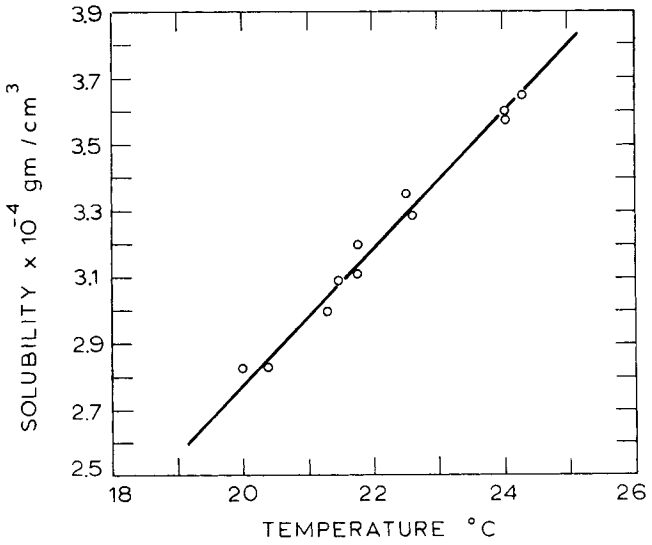

Fig. 3. Solubility of ethyl salicylate in water as a function of temperature.

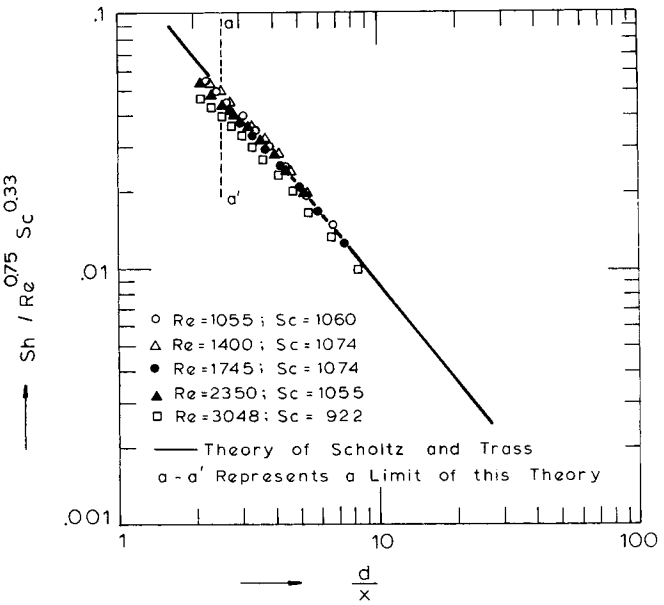

Fig. 4. Comparison of experimental and theoretical local mass transfer coefficients.

viation from the theoretical line, the duration of the experiment was a large fraction of the constant rate period as predicted by the methods of Macleod and Todd (1973). It is shown by Macleod and Ruess that these methods, applied to the ethyl salicylate/water system used here, predict values of the constant rate period nearly three times as great as those found experimentally. This discrepancy is probably due to the nonideality of the ester/water system. In any experiment having a duration more than half the predicted period, therefore, the mass transfer rate will decline significantly as transfer proceeds, and the time-averaged value of this rate will appear low. For the present experimental arrangement, the predicted constant rate period (which is a decreasing function of the mass transfer flux), falls with increasing Reynolds number and diminishing x/d. The deviation of our data points from the theoretical line increases systematically in the same sense. For deviations of 5%, for example, we find that t/t', the ratio of the duration of the experiment to the local value of the constant rate period predicted by the methods of Macleod and Todd (1973), was 0.55 to 0.57; for 17% deviation, this ratio t/t' was 0.72. These figures are in agreement with the measurements of Macleod and Ruess of the discrepancy between actual and predicted constant rate periods for this ester/water system.

The practical significance of these deductions is that this particular experimental system is characterized by an inconveniently short constant rate period where the mass transfer rate is high, that is, in the inner parts of the wall-jet region and at higher jet Reynolds numbers. For this reason no attempt was made here to explore the jet impingement and transition regions, where the mass transfer rates are higher still. These inner regions have been explored in our air-jet experiments (Kapur and Macleod, 1974) for which the constant rate period is substantially longer under given experimental conditions; and they could readily be investigated in liquid-jet experiments if a swelling agent of lower solubility were used or if the physical size of the apparatus were increased.

CONCLUSIONS

Our results demonstrate that a holographic technique of local mass transfer rate determination at solid surfaces, previously developed by us for use with air-flow systems of Schmidt number of the order unity, is equally applicable to systems of Schmidt number of the order 10^3 using water as the experimental fluid. This technique, already shown to be an exceptionally precise, powerful, and convenient means of investigating spatial variations of transfer rate, is evidently suitable also for determining the influence of diffusivity on convective mass transfer rates over a wide range of values of this parameter.

Using this holographic method we have shown that measured local mass transfer coefficients at a plane surface on which a submerged jet impinges normally are, for the wall-jet region, in good agreement with the theory of Scholtz and Trass. Taken together with our earlier results, using the same method for a similar system having a Schmidt number three orders of magnitude less, this represents strong evidence for the validity of the theory over the range of radial distances corresponding to the wall-jet region. In particular, these results confirm the predicted functional effects on transfer rate both of distance from the jet axis and of diffusivity in the fluid stream for a wide range of these variables.

For the particular mass transfer system employed here, in which ethyl salicylate is eluted by the water stream from a swollen coating of silicone rubber, it is found that the rate of coating recession ceases to be sensibly constant after a period substantially less than that predicted on the assumption that the water/ester system behaves as an ideal solution. This result, which accords with those of Ruess from a more detailed investigation of the time variation of elution rate for this system, does not fundamentally affect the utility of the experimental technique but must be taken into account in the choice of swelling agent and the design of experiments in which such methods are applied to mass transfer measurement at solid/water interfaces.

ACKNOWLEDGMENT

We wish to thank the Heat Transfer Group of R.D.L., Windscale Works, U.K.A.E.A., for its financial support for this project, and particularly for the maintenance of D. N. Kapur.

NOTATION

d = diameter of the nozzle, cm
D = diffusion coefficient of ethyl salicylate in water, cm^2/s
k = local mass transfer coefficient at radial location x, cm/s
t = elapsed time from commencement of transfer, s
t' = constant rate period predicted by the methods of Macleod and Todd, s
u = nozzle exit velocity, cm/s
x = radial distance from stagnation point, cm
Re = Reynolds number, ud/ν
Sc = Schmidt number for ethyl salicylate/water system ν/D
Sh = Sherwood number, kd/D

Greek Letters

ν = kinematic viscosity of water, cm^2/s

LITERATURE CITED

Kapur, D. N., "The profilometric determination of mass transfer coefficients by holographic interferometry," Ph.D. thesis, *Nature, Phys. Sci. Lond.*, **237**, Univ. Edinburgh, Scotland (1973).

———., and N. Macleod, "Determination of local mass transfer coefficients by holography," *Nature, Phys. Sci. Lond.*, **237**, 57 (1972).

———., "The determination of local mass transfer coefficients by holographic interferometry," *Intern. J. Heat. Mass Transf.*, **17**, 1151 (1974).

Macleod, N., and D. N. Kapur, "A kinematically designed mount for the precise location of specimens for holographic interferometry," *J. Phys. E.:Scientific Instruments*, **6**, 423 (1973).

Macleod, N., and T. Ruess, "The radial transfer of mass to an axial stream of liquid between coaxial rotating cylinders," *Chem. Eng. Sci.*, in press.

Macleod, N., and R. B. Todd, "The experimental determination of wall-fluid mass transfer coefficients using plasticised polymer surface coatings," *Intern. J. Heat Mass Transfer*, **16**, 485 (1973).

Scholtz, M. T., and O. Trass, "Mass transfer in the laminar radial wall jet," *AIChE J.*, **9**, 548 (1963).

Manuscript received June 6, 1974; revision received and accepted September 25, 1974.

An Analysis of Turbulent Pipe Flow with Viscosity Variation in the Wall Region

G. A. HUGHMARK

Ethyl Corporation
Baton Rouge, Louisiana 70821

A paper and notes by the author (1971, 1972, 1973) showed that wall region and transition region mass transfer for turbulent pipe flow are represented by the equations

$$k^+_{EW} = 0.065\ N_{Sc}^{-2/3} \tag{1}$$

and

$$k^+_{ET} = 0.0615\ N_{Sc}^{-1/2} \tag{2}$$

These equations are shown to be consistent with the wall region frequency relationship

$$\frac{u^{*2}\,t}{\nu} = 338 \tag{3}$$

This note presents an extension of this work to heat transfer with variable viscosity in the wall region.

NEWTONIAN FLUIDS

Equation (2) corresponds to the penetration model with the frequency from Equation (3). This can be expressed in heat transfer terms to represent the transition region properties

$$\frac{h}{\rho_T\, C_{pT}} = 2\sqrt{\frac{k_T}{\pi \rho_T\, C_{pT}\, t}} \tag{4}$$

Substitution of Equation (3) which represents bulk fluid properties provides

$$\frac{h}{\rho_T\, C_{pT}} = 0.0615\ u^*\,(N_{PrT})^{-1/2}\,(\nu_T/\nu_b)^{1/2} \tag{5}$$

Equation (2) reduces to the mass transfer analog of Equation (5) for isothermal conditions. Equation (5) would be expected to represent the transition region and to be applicable to heat transfer data with significant resistance in this region.

The momentum analog is useful in evaluating the kinematic viscosity ratio for Equation (5). Isothermal turbulent flow results in an essentially constant kinematic viscosity in the wall and transition regions. Momentum equations for isothermal and nonisothermal flow are

$$\frac{\tau}{\rho} = 0.332\ U^2_{\infty i}\sqrt{\frac{\nu}{U_{\infty i}\,x}} \tag{6}$$

and

$$\frac{\tau}{\rho} = 0.332\ U^2_{\infty ni}\sqrt{\frac{\nu_T}{U_{\infty ni}\,x}} \tag{7}$$

Combination of Equations (3), (6), and (7) yields

$$U^+_{\infty ni} = (\nu_b/\nu_T)^{1/3}\ U^+_{\infty i} \tag{8}$$

with the assumption that Equation (3) represents the bulk kinematic viscosity. The dimensionless shearing stress for a developing boundary layer on a flat plate leads to the friction factor relationship

$$f = \frac{0.664}{\sqrt{\dfrac{U_\infty\, x}{\nu}}} \tag{9}$$

Friction factor equations for isothermal and nonisothermal flow with substitution of Equation (3) are

$$f_i = \frac{0.036}{\sqrt{U^+_{\infty ni}}} \tag{10}$$

$$f_{ni} = \frac{0.036}{\sqrt{U^+_{\infty ni}\ \nu_b/\nu_T}} \tag{11}$$